

Sonochemically Produced ZnS-Coated Polystyrene Core–Shell Particles for Use in Photonic Crystals

M. L. Breen,^{*,†,‡} A. D. Dinsmore,^{‡,§} R. H. Pink,^{†,||} S. B. Qadri,[†] and B. R. Ratna[†]

Naval Research Laboratory, 4555 Overlook Avenue, SW, Washington, D.C. 20375-5320,
Harvard University, Division of Engineering and Applied Sciences, 9 Oxford Street,
Cambridge, Massachusetts 02138, and George Mason University, 4400 University Drive,
Fairfax, Virginia 22030-4444

Received August 10, 2000. In Final Form: October 27, 2000

Zinc sulfide films were grown on carboxyl-modified polystyrene microspheres (PS-CO₂) through sonochemical deposition in an aqueous bath containing zinc acetate and sulfide, released through the hydrolysis of thioacetamide. The resulting particles were "optically hollow", due to a large refractive index contrast between the core and shell materials. Continuous, uniform films were obtained after 3–4 h and reached a maximum thickness of 70–80 nm after 13 h of growth, as characterized by transmission electron microscopy (TEM). Aggregation was minimized by subsequent modification of the core–shell particles with mercaptoacetic acid to increase their surface charge and produce good colloidal suspensions. Oscillations in the optical spectra of dilute suspensions of the particles were indicative of interference patterns as expected from Mie light scattering calculations. X-ray diffraction (XRD) patterns match the zinc blende structure of ZnS and indicate a compression in the crystal lattice ($a = 5.305 \pm 0.037 \text{ \AA}$), as compared to the bulk material ($a = 5.406 \text{ \AA}$). Hollow ZnS shells were formed by annealing the core–shell particles in a thermal gravimetric analysis (TGA) oven, at 400 °C. A 34% weight loss was observed upon heating, a value approximately equal to that of the polystyrene core. The hollow shells remained intact and readily resuspended in water. Both core–shell and hollow ZnS particles self-assemble to form well-ordered, hexagonal close-packed layers.

Introduction

Tremendous activity in the nascent field of photonic band gap materials (PBG) has ensued since their utility was first demonstrated by Yablonovitch in 1987 for the microwave regime.¹ Since then, photonic band gaps have been demonstrated in one- and two-dimensions at the optical and infrared wavelengths.² Some success has been achieved through lithographic methods to produce three-dimensional PBG's for infrared light,^{3,4} but the pursuit of a microscopically ordered PBG, with large refractive index contrast active in the visible range, continues to be a challenging endeavor. Using standard microelectronic fabrication techniques, structures with periodic features of 1–2 μm were prepared in an arrangement which resulted in a band gap for infrared light of 10–14.5 μm wavelengths.⁴ Samples made through this layer-by-layer method exhibit adequate spatial resolution but are difficult to prepare in extended 3-D structures. More importantly, to produce crystals with PBG's in the visible range it will be necessary to pattern features at the submicrometer level. This degree of structural resolution stretches the limits of lithographic techniques and would be prohibitively expensive to achieve.

Colloidal self-assembly has been utilized as a process to form 3-D periodic structures because of its simplicity.⁵ A variety of methods have been explored to make photonic crystals out of porous, ceramic materials templated to submicrometer balls of SiO₂,⁶ polystyrene latex,^{7,8} and oil emulsions,⁹ arranged into 3-D ordered structures. Solutions of metal alkoxides^{7,8} or phenolic resins⁶ were coated over the templates, filling the interstitial spaces. The metal alkoxides were hydrolyzed to metal oxides, and the phenolic resin was reduced to carbon graphite. The materials were annealed to increase the density of their ceramic/carbon matrixes. Unfortunately, the resulting strain from shrinkage distorted the lattices and substantially degraded the optical properties of the colloidal crystals. Recently, a silicon photonic crystal with a complete band gap near 1.5 μm was prepared using a close-packed opal crystal of silica spheres.¹⁰ The voids in this crystal were backfilled with silicon using CVD, and the silica template was subsequently acid-etched to produce a 3-D periodic, inverse fcc crystal of silicon.

In this paper we describe a process to achieve a similar inverse structure using zinc sulfide/polystyrene core–shell (c–s) particles. Zinc sulfide, with a high refractive index ($n_{488} = 2.43$) and relatively low absorption in the visible spectrum, is an attractive material for use in photonic crystals. Also, since ZnS can be prepared in an aqueous

[†] Naval Research Laboratory.

[‡] National Research Council Research Associate.

[§] Harvard University.

^{||} George Mason University.

(1) Yablonovitch, E. *Phys. Rev. Lett.* **1987**, *58*, 2059.

(2) Foresi, J. S.; Villeneuve, P. R.; Ferrera, J.; Thoen, E. R.; Steinmeyer, G.; Fan, S.; Joannopoulos, J. D.; Kimerling, L. C.; Smith, H. I.; Ippen, E. P. *Nature* **1997**, *390*, 143.

(3) Noda, S.; Yamamoto, N.; Kobayashi, H.; Okano, M.; Tomoda, K. *Appl. Phys. Lett.* **1999**, *75*, 905–907.

(4) Lin, S. Y.; Fleming, J. G.; Hetherington, D. L.; Smith, B. K.; Biswas, R.; Ho, K. M.; Sigalas, M. M.; Zubrzycki, W.; Kurtz, S. R.; Bur, J. *Nature* **1998**, *394*, 251–253.

(5) Xia, Y.; Gates, B.; Yin, Y.; Lu, Y. *Adv. Mater.* **2000**, *12*, 693.

(6) Zakhidov, A. A.; Baughman, R. H.; Iqbal, Z.; Cui, C.; Khayrullin, I.; Dantas, S. O.; Marti, J.; Ralchenko, V. G. *Science* **1998**, *282*, 897–901.

(7) Wijnhoven, J. E. G. J.; Vos, W. L. *Science* **1998**, *281*, 802.

(8) Holland, B. T.; Blanford, C. F.; Stein, A. *Science* **1998**, *281*, 538–540.

(9) Imhof, A.; Pine, D. J. *Nature* **1997**, *389*, 948.

(10) Blanco, A.; Chomski, E.; Grabtchak, S.; Ibisate, M.; John, S.; Leonard, S. W.; Lopez, C.; Meseguer, F.; Miguez, H.; Mondia, J. P.; Ozin, G. A.; Toader, O.; Driel, H. *Nature* **2000**, 437–440.

bath, the synthetic route is relatively inexpensive and environmentally benign. A unique feature of the core-shell approach is its ability to provide a structure in which the high- n material is continuous (within each sphere) and present in a low overall volume fraction. This allows for an optimum fraction of 0.2–0.3 of high refractive material as prescribed by theoretical calculations.^{11,12} We further show that it is possible to remove PS before self-assembling the photonic crystal, thus eliminating the issues associated with lattice shrinkage and post-acid etching. This simple and inexpensive approach enables the growth of large, photonic crystals and can be extended to other high refractive index materials, such as PbS.

Experimental Section

Materials. Zinc acetate (99.99%) and thioacetamide (99+%) were purchased from Aldrich and used without further purification. Several sizes of carboxylate-modified polystyrene (PS-CO₂) microspheres were obtained from Seradyn (Indianapolis, IN). Microspheres were used, as is, without removing the proprietary surfactant. The surfactant was found not to interfere with deposition, and removing the surfactant lead to increased aggregation of the particles. Ultrasonic irradiation was delivered by a 0.25 in. titanium, tapered microtip probe attached to a 20 kHz \pm 50 Hz, 600 W power source (Ace Glass, Vineland, NJ).

Preparation of ZnS/PS-CO₂. Zinc sulfide was sonochemically deposited on carboxyl-modified, polystyrene (PS-CO₂) microspheres using a modified method adapted from previously published work with silica particles.¹³

In a 50 mL round-bottom flask was combined Zn(Ac)₂ (300 mg, 1.63 mmol) and 50 mL of Milli-Q water. The solution was agitated in a sonic bath for 30 s or until all the metal salt was dissolved. An aliquot of the suspended PS-CO₂ beads (50 mg diluted to 1.5 mL) was added, followed by thioacetamide (123 mg, 1.63 mmol). A sonic probe was immersed in the reaction solution which was then pulsed (0.5/0.5 s on/off) for 6 h (18% power or 108 W). The final product was washed several times with Milli-Q water, coated with 3-mercaptopoacetic acid (0.1 g, 900 mmol), and resuspended in water (10–12 mL) adjusted to pH = 10 with 1.0 M KOH.

To determine film growth over time, aliquots of the reaction solution (0.50 mL) were collected prior to sonication and then at 1 h intervals: 1, 2, ... 8, and 13 h. Each aliquot was washed several times with Milli-Q water, centrifuged to remove the supernatant, and then resuspended in water.

Self-Assembly of Core-Shell Particles. A process of convective assembly was used to direct the orientation of ZnS/PS-CO₂ core-shell particles on the surface of glass or polished silicon wafers.^{14–16} An aqueous suspension of the particles was drawn out of a solution reservoir held between a glass slide and cover glass by capillary action. The reservoir was translated across the substrate at approximately 23 μ m/s, depositing a thin film of c-s solution on the substrate surface. Particle assemblies were allowed to air-dry.

Annealing of ZnS/PS-CO₂ Particles. Suspensions of the core-shell particles were dried in a vacuum desiccator (80 °C). The dry powder was heated in a thermal gravimetric analysis (TGA) oven under a stream of nitrogen gas. Temperature was increased at 2 °C/min and then held for 1 h at each 100 °C increment up to 600 °C.

Characterization. Particle suspensions were studied with a Nikon Optihot optical microscope. Transmission electron micrographs of the ZnS/PS-CO₂ core-shell particles were taken

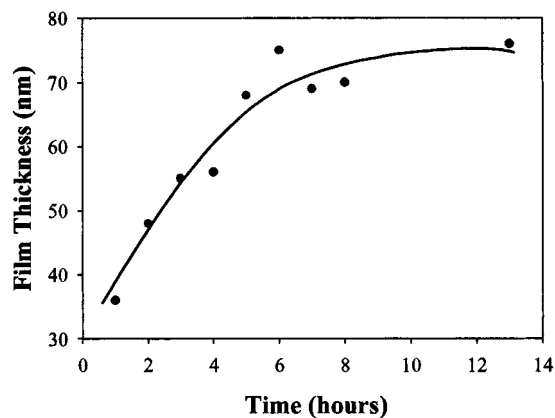


Figure 1. ZnS film growth on 0.827 μ m polystyrene spheres vs deposition time.

with a Hitachi H-8100 TEM (accelerating voltage = 200 kV). Shell thickness was estimated from TEM micrographs. Light-scattering of the particles in aqueous solutions was analyzed from UV/vis spectra using a Cary 4G scanning spectrometer. X-ray diffraction patterns were collected on a Rigaku two-circle diffractometer using Cu K α radiation from a Rigaku 12 kW rotating anode X-ray generator. The peaks were analyzed with PeakFit, spectroscopic analysis software used to obtain peak positions, peak widths, and other structural information. Particles were further studied by LEO 1550 scanning electron microscope (SEM).

Results and Discussion

The thickness of zinc sulfide shells was estimated from TEM micrographs. Since the electron density of ZnS is so much greater than that of polystyrene, the metal sulfide shell appeared as a dark ring around a core of lighter material. After 1 h of sonication, the surfaces of the 0.827 μ m PS-CO₂ beads were completely covered with ZnS. However, the films were not smooth and uniform before 3–4 h of growth had accumulated. Little or no film growth was observed after 6 h (Figure 1). Similar rates of deposition were recorded for 0.441 μ m PS-CO₂ beads.

To produce well-ordered crystals of colloidal particles, the particles must remain in a homogeneous suspension prior to self-assembly. Therefore, it is critical that random aggregation is strictly curtailed. As purchased, the polystyrene spheres are modified with a carboxylic acid group to give them a repulsive surface charge. In contrast, ZnS-coated particles have a surface charge close to neutral. Therefore, mercaptoacetic acid was added to reduce the surface charge of the c-s particles and improve their monodispersity while in suspension. The effectiveness of this step was directly visible by optical microscopy. Particles coated with mercaptoacetic acid remained suspended in aqueous solutions for longer periods of time and were more difficult to precipitate by centrifuge.

X-ray Powder Diffraction Pattern. Analysis of the ZnS/0.441 μ m PS-CO₂ core-shell particles confirmed that deposited films assumed the zinc blende structure (Figure 2a). Information on the lattice strain and crystallite size was obtained from the (111), (220), and (311) diffraction peaks. After correcting for instrumental broadening, the average crystallite size, calculated from full widths at half-maximum (fwhm) of the diffraction peaks and Scherrer's formula,¹⁷ was found to be 25 Å or 2.5 nm. A least-squares refinement of the data revealed a lattice parameter of $a = 5.305 \pm 0.037$ Å, which is 1.9% smaller than the reported

(11) Biswas, R.; Sigalas, M. M.; Subramania, G.; Ho, K.-M. *Phys. Rev. B* **1998**, *57*, 3701.

(12) Lin, S.-Y.; Chow, E.; Hietala, V.; Villeneuve, P. R.; Joannopolous, J. D. *Science* **1998**, *282*, 274.

(13) Dhas, N. A.; Zaban, A.; Gedanken, A. *Chem. Mater.* **1999**, *11*, 806.

(14) Dimitrov, A. S.; Nagayama, K. *Langmuir* **1996**, *12*, 1303–1311.

(15) Kralchevsky, P. A.; Nagayama, K. *Adv. Colloid Interface Sci.* **2000**, *85*, 145–192.

(16) Maenosono, S.; Dushkin, C. D.; Yamaguchi, Y.; Nagayama, K.; Tsuji, Y. *Colloid Polym. Sci.* **1999**, *277*, 1152–1161.

(17) Cullity, D. *Elements of X-ray Diffraction*; Addison-Wesley Pub. Inc.: Reading, MA, 1978.

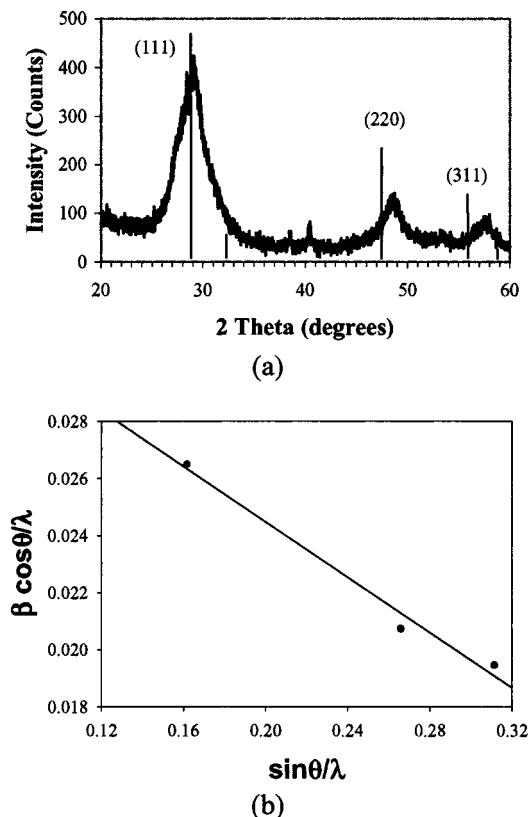


Figure 2. (a) X-ray powder diffraction of ZnS/0.441 μm polystyrene spheres vs simulated line spectra of bulk ZnS. (b) Negative slope in plot indicates compressive strain in ZnS crystal lattice.

bulk value of $a = 5.406 \text{ \AA}$ for zinc blende ZnS (PDF 05-0566).

The fwhm's can be expressed as a linear combination of the contributions from the lattice strain and crystallite size through the following equation:

$$\frac{\beta \cos \theta}{\lambda} = \frac{1}{\epsilon} + \frac{\eta \sin \theta}{\lambda} \quad (1)$$

Here β is the measured fwhm in radians, θ is the Bragg angle of the diffraction peak, λ is the X-ray wavelength, ϵ is the effective particle size, and η is the effective strain.^{18,19} A plot of $\beta \cos \theta/\lambda$ versus $\sin \theta/\lambda$ is shown in Figure 2b. On the basis of eq 1, the extrapolated crystallite size was 29 \AA , compared with 25 \AA calculated from Scherrer's equation, which does not consider strain. The slope of the fitted line is negative, indicating the presence of compressive strain in the ZnS crystal lattice. This corroborates the evidence of strain indicated above by the reduced lattice parameter of the crystals.

Powder patterns for the series of samples collected between 0 and 6 h of film deposition on 0.827 μm PS-CO₂ microspheres were also generated (Figure 3). With time and increasing film thickness, peak positions did not shift nor did peak widths decrease or increase. This indicates that lattice dimensions and crystallite size for the particles were constant throughout the growth experiment. Crystallite size for the ZnS/0.827 μm core–shell particles was

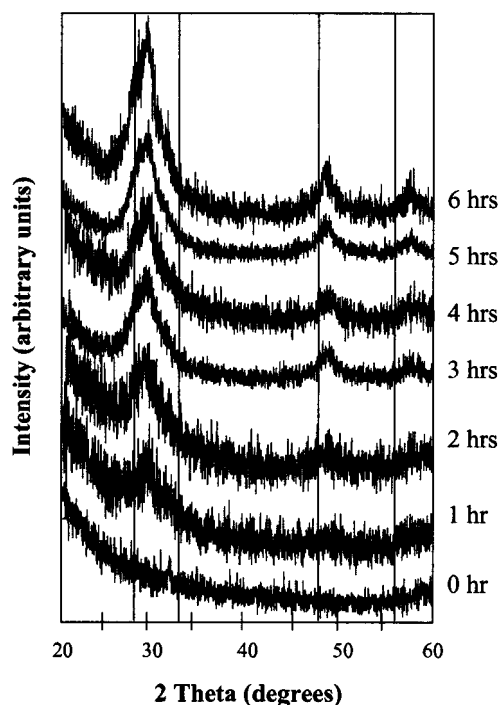


Figure 3. X-ray powder diffraction patterns of ZnS/0.827 μm polystyrene core–shell particles at 0–6 h of film growth.

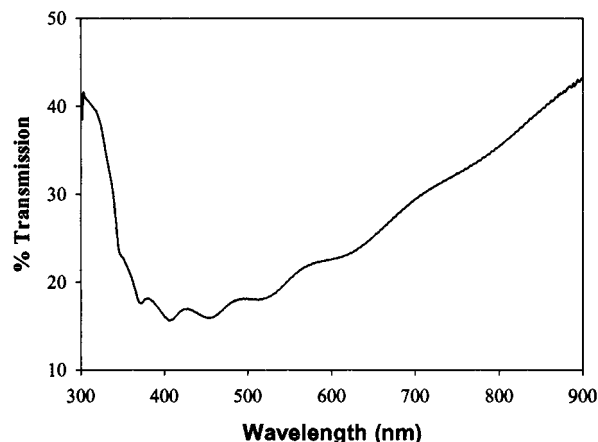


Figure 4. UV/vis spectrum of ZnS/0.441 μm polystyrene core–shell particles (13 h). Oscillations show interference patterns between core and shell materials.

similar to the value of 25 \AA calculated for the smaller ZnS/0.441 μm particles.

UV/Vis Spectroscopy. A very broad scattering peak near 400 nm was observed for plain 0.441 μm PS-CO₂. The spectra of the corresponding core–shell particles was superimposed with a periodic oscillation which increased in frequency with decreasing wavelength (Figure 4). Similar oscillations were seen in the spectra of ZnS/0.827 μm PS-CO₂ core–shell particles which were collected for a range of reaction times (Figure 5). This phenomenon is caused by interference patterns between ZnS and the polystyrene core material. It is a significant observation which was predicted using Mie light-scattering theory²⁰ but has not been previously observed for similar c–s composites.¹³ Oscillations increased in amplitude and the transmission window underwent a red shift with increasing shell thickness (Figure 5). It is not clear why the

(18) Qadri, S. B.; Skelton, E. F.; Hsu, D.; Dinsmore, A. D.; Yang, J.; Gray, H. F.; Ratna, B. R. *Phys. Rev. B: Condens. Matter* **1999**, *60*, 9191–9193.

(19) Qadri, S. B.; Yang, J. P.; Skelton, E. F.; Ratna, B. R. *Appl. Phys. Lett.* **1997**, *70*, 1020–1021.

(20) Bohren, C. F.; Huffman, D. R. *Absorption and Scattering of Light by Small Particles*; John Wiley and Sons: New York, 1983.

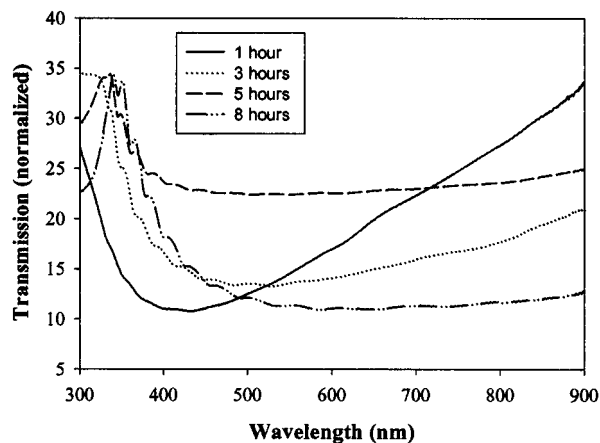


Figure 5. UV/vis light scattering, ZnS/0.827 μm polystyrene vs deposition time. The “red shift” corresponds with theoretical predictions for Mie light scattering with increasing film thickness.

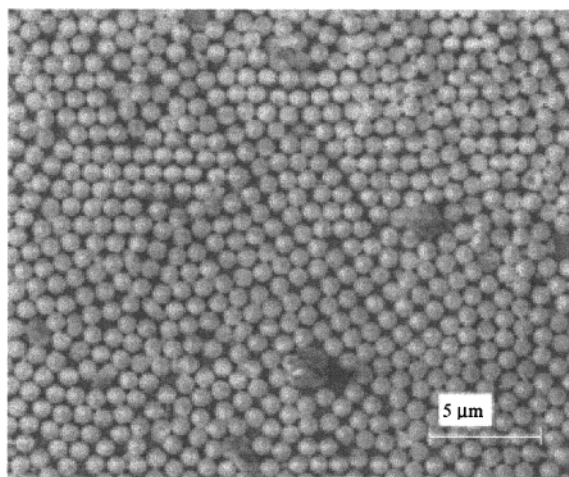


Figure 6. Self-assembly of ZnS/0.827 μm polystyrene core-shell particles on silicon illustrating hexagonal packing.

oscillations in general were larger in magnitude for the 0.827 μm vs the 0.441 μm c-s microspheres with similar ZnS shell thicknesses. Mie calculations were used to determine the approximate refractive index of the ZnS from shell thickness (TEM) and light scattering (UV/vis) data. A value of $n = 2.0$ was found, slightly below $n = 2.4$ for bulk ZnS. This is likely due to the porous nature of the ZnS films, which are more aggregates of nanocrystalline particles than polycrystalline films.

Self-Assembly of Core-Shell Particles. Monolayer films of the core-shell particles showed hexagonal-packing over large areas (Figure 6). Ongoing studies are focusing on the development of improved techniques for better controlling particle assembly and reducing the number of defects in three-dimensional structures.

Annealed Core-Shell Particles. Up to 290 $^{\circ}\text{C}$, a small weight loss (7–8%) was observed during TGA probably due to the evaporation of residual moisture in the sample (Figure 7). Between 290 and 400 $^{\circ}\text{C}$, a weight loss of 34% was measured over a period of roughly 50 min. This corresponds to the calculated weight fraction of polystyrene contained in the c-s particles. The weight of the sample was unchanged from 400 to 600 $^{\circ}\text{C}$. While bulk ZnS undergoes a phase transition from zinc blende (cubic) to its wurtzite (hexagonal) structure at 1050 $^{\circ}\text{C}$, nanoparticles of ZnS were previously observed to undergo the same transition at temperatures as low as 500 $^{\circ}\text{C}$.¹⁸ Contrastingly, XRD patterns for the hollow ZnS micro-

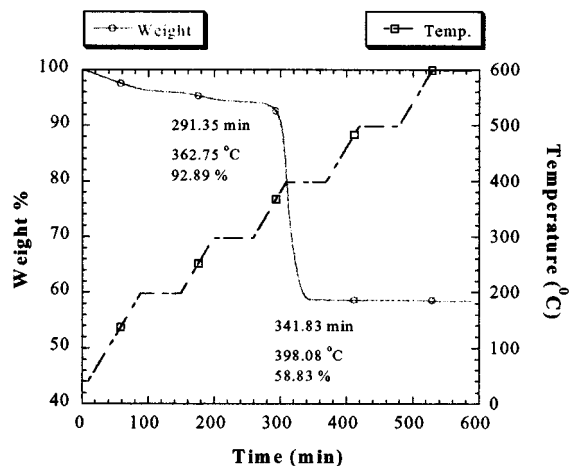


Figure 7. Thermal gravimetric analysis of ZnS/0.827 μm polystyrene core-shell particles. The weight percent lost approximates the mass of the polymer core at 400 $^{\circ}\text{C}$.

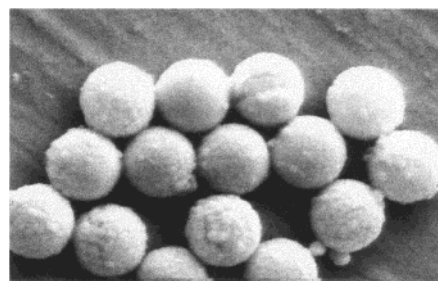


Figure 8. Self-assembly of hollow ZnS microspheres.

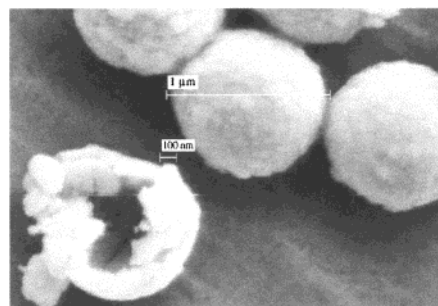


Figure 9. “Exploded” hollow ZnS microsphere.

spheres differed little from those collected prior to annealing, thus indicating no structural phase transitions occurred. To be more succinct, while it was previously observed¹⁸ that a powder of 2.5 nm crystallites underwent a phase transition at 500 $^{\circ}\text{C}$ the 70–80 nm aggregate films of 2.5 nm crystallites, described in this experiment, did not.

Annealed microspheres resuspended readily in water. SEM photographs showed that the hollow particles remained intact and were unchanged in their dimensions (Figure 8). Hexagonal close-packed assemblies, seen in SEM photographs of the hollow shells, indicate that well-ordered inverse fcc lattices could be obtained. A few particles did rupture, revealing their empty interiors (Figure 9).

Conclusions

Optically hollow zinc sulfide/polystyrene core-shell particles were sonochemically prepared in an aqueous bath. The uniform spherical shape of the particles facilitate the three-dimensional assembly of the crystalline matrixes with long-range periodicity. Intact, hollow ZnS shells were

obtained by heating the particles to remove their polystyrene cores. These truly, optically hollow shells should have an even higher refractive index contrast than the c-s particles. Interference patterns observed by optical spectroscopy demonstrate that particles consisting of two layers of material with distinctively different refractive indices were produced. Compression of the ZnS lattice from that of the bulk material indicates prominent surface, strain forces which could have important effects on the optical qualities of thin film refractive materials.

Acknowledgment. This work was supported by the Office of Naval Research and the National Research Council through their Research Associateships Program. Special thanks to Joseph Perrin (Naval Research Laboratory) for the TGA analysis and Grant Blouse (Henry Ford Health System) for his advice on surface-capping agents.

LA0011578